Theory and design of a free-electron maser with two-dimensional feedback driven by a sheet electron beam

N. S. Ginzburg, N. Yu. Peskov, and A. S. Sergeev
Institute of Applied Physics, Russian Academy of Sciences, N. Novgorod, Russia

A. D. R. Phelps, I. V. Konoplev, G. R. M. Robb, and A. W. Cross
University of Strathclyde, Glasgow, United Kingdom

A. V. Arzhannikov and S. L. Sinitsky
Institute of Nuclear Physics, Russian Academy of Sciences, Novosibirsk, Russia

(Received 14 December 1998)

The use of two-dimensional Bragg resonators of planar geometry, realizing two-dimensional (2D) distributed feedback, is considered as a method of producing spatially coherent radiation from a large sheet electron beam. The spectrum of eigenmodes is found for a 2D Bragg resonator when the sides of the resonator are open and also when they are closed. The higher selectivity of the open resonator in comparison with the closed one is shown. A time-domain analysis of the excitation of an open 2D Bragg resonator by a sheet electron beam demonstrates that a single-mode steady-state oscillation regime may be obtained for a sheet electron beam of width 100–1000 wavelengths. Nevertheless, for a free-electron maser (FEM) with a closed 2D Bragg resonator, a steady-state regime can also be realized if the beam width does not exceed 50–100 wavelengths. The parameters for a FEM with a 2D planar Bragg resonator driven by a sheet electron beam based on the U-2 accelerator (INP RAS, Novosibirsk) are estimated and the project is described. [S1063-651X(99)04207-5]

PACS number(s): 41.60.Cr, 52.75.Ms, 84.40.Fe, 84.40. Ik

I. INTRODUCTION

In recent years many successful experiments have been carried out on free electron masers (FEM's), which utilize conventional Bragg resonators [1–5]. Such resonators are constructed by machining single periodic corrugations on the inner wall of the waveguide. However, in all previous experiments the diameter of the microwave systems used (D) does not exceed the wavelength of the radiation (λ) by more than a factor $D/\lambda \approx 2-4$ and the output power produced was not more than 50 MW. Further increase in the transverse dimensions of the 1D Bragg cavity would result in the loss of its selectivity.

However, for some applications it is attractive to achieve gigawatt power levels of millimeter wave radiation by utilizing a large high-current sheet beam as the FEM driver. The use of such a beam makes it possible to increase the total beam power and, correspondingly, the microwave power while still keeping the current and radiation density per unit transverse size constant. Indeed, at the U-2 accelerator (Budker Institute of Nuclear Physics, RAS, Novosibirsk) a microsecond relativistic sheet electron beam with electron energy of 1 MV, current per unit transverse size (linear current density) of 1 kA/cm, and transverse size up to 140 cm was generated [6,7]. The power of this beam is tens of gigawatts and its energy is up to 0.5 MJ.

The main problem for the FEM driven by large size sheet beams is producing coherent radiation from different parts of the electron beam. To solve this problem, two-dimensional (2D) distributed feedback has been recently proposed [8–10]. 2D distributed feedback may be realized in a Bragg resonator which consists of two metal plates with a doubly periodical corrugation. On this corrugation mutual scattering of electromagnetic energy fluxes propagating in forward, backward, and transverse directions relative to the direction of electron beam propagation takes place. The additional transverse electromagnetic energy fluxes should synchronize radiation from different parts of the large sheet electron beam.

This paper is devoted to theoretical consideration of the novel scheme of the FEM with 2D Bragg resonators of planar geometry. In Sec. II the basic model and main equations for electromagnetic (e.m.) waves scattering on the double-corrugated Bragg structure are presented. In Sec. III properties of the open planar 2D Bragg resonator are considered. In Sec. IV we investigate the excitation of such a resonator by a sheet relativistic electron beam and study of the build-up oscillations. In Sec. V the influence of external reflections of the transverse e.m. fluxes on the FEM operation is studied. In Sec. VI a project of 4-mm superpower FEM with a 2D planar Bragg resonator driven by a 140 cm sheet relativistic electron beam is discussed.

II. MODEL AND BASIC EQUATIONS

The planar 2D Bragg resonator consists of two metal plates corrugated surface defined by

$$a = a_1[\cos(\overline{h}_x x - \overline{h}_z z) + \cos(\overline{h}_x x + \overline{h}_z z)] \qquad (1)$$

inside the rectangular area of width l_x, length l_z, and separated by distance a_0 (Fig. 1). In Eq. (1), $\overline{h}_x = \overline{h}\sin\varphi$, $\overline{h}_z = \overline{h}\cos\varphi$, $\overline{h} = 2\pi/d$, d is the corrugation period, a_1 is the corrugation depth, and 2φ is the angle between the grating vectors $\vec{h}$ [Fig. 1(c)]. Assuming $\overline{h}a_1 \ll 1$, we will describe the

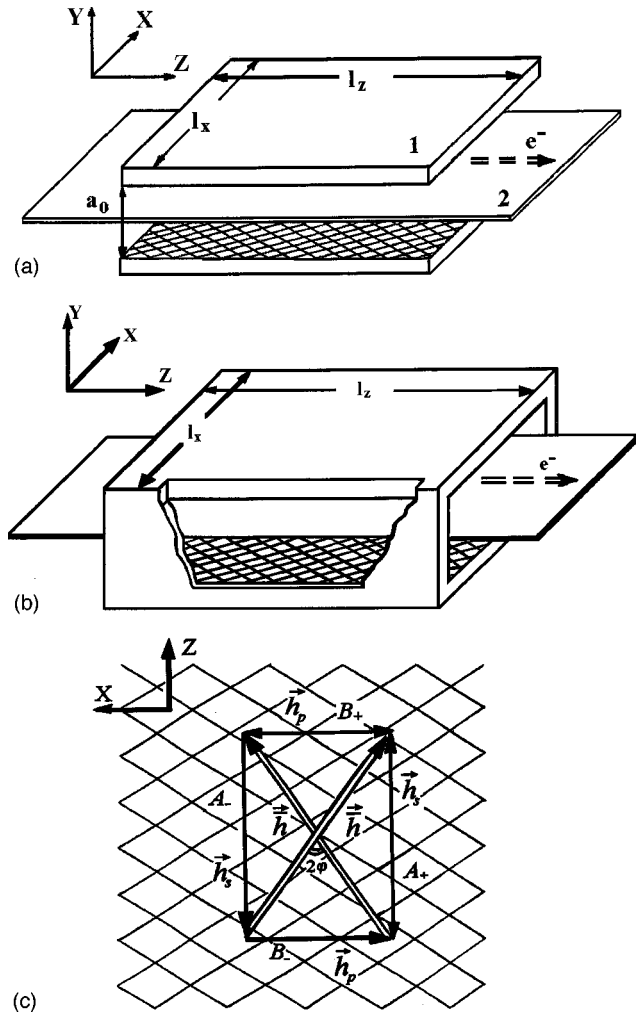

FIG. 1. Schematic diagram of FEL oscillator with an open (a) and closed (b) planar 2D Bragg resonator driven by a sheet electron beam. Diagram illustrating the scattering of the partial waves on the 2D Bragg grating (c) ($\vec{h}$ are the wave vectors of the partial waves $\mathcal{A}_\pm$ and $\mathcal{B}_\pm$, $\vec{\bar{h}}$ are the grating vectors).

field within the resonator in the form of four coupled waves: $\mathcal{A}_\pm$ is propagating in $\pm z$ directions and having s field variations over the transverse y coordinate and $\mathcal{B}_\pm$ is propagating in $\pm x$ directions and having p field variations over y,

$$\vec{E}=\mathrm{Re}[(\mathcal{A}_+\vec{E}_s^0 e^{-h_s z}+\mathcal{A}_-\vec{E}_s^0 e^{ih_s z}+\mathcal{B}_+\vec{E}_p^0 e^{-ih_p x}+\mathcal{B}_-\vec{E}_p^0 e^{ih_p x})e^{i\omega t}]. \tag{2}$$

Here $\mathcal{A}_\pm(x,z)$ and $\mathcal{B}_\pm(x,z)$ are slow functions of the x and z coordinates $h_j=\sqrt{\omega^2/c^2-g_j^2}$, $g_j=j\pi/a_0$ is the transverse (over the y axis) wave number, $j=0,1,2,\ldots$, $\vec{E}_{s,p}^0(y)$ are functions describing the spatial wave profile along the y coordinate, which coincide with one of the eigenmodes of the planar waveguide:

$$\vec{E}_j^0=i\vec{x}_0\frac{\omega}{c}\sin(g_j y) \tag{3a}$$

for TE modes, and

$$\vec{E}_j^0=\vec{z}_0 g_j\sin(g_j y)-i\vec{y}_0 h_j\cos(g_j y) \tag{3b}$$

for TM modes, including the TEM mode (which corresponds to $j=0$).

The wave vectors of the partial waves satisfy the Bragg resonance condition when scattering on the grating:

$$\vec{h}_s-\vec{h}_p=\vec{\bar{h}}. \tag{4}$$

If the grating vectors are perpendicular to each other ($2\varphi=\pi/2$, $\bar{h}_x=\bar{h}_z$) all the partial waves will possess the same longitudinal wave numbers and the same numbers of transverse variations ($s\equiv p$), otherwise the waves $\mathcal{A}_\pm$ and $\mathcal{B}_\pm$ have the different transverse variation indices.

Substituting Eq. (2) into the Helmholtz equation with a periodic boundary condition imposed at the corrugated plate surface (1) and averaging, we obtain the following set of equations for the slow amplitudes $\mathcal{A}_\pm,\mathcal{B}_\pm$:

$$e^{\mp i\Lambda_s z}\frac{\partial\mathcal{A}_\pm}{\partial z}\mp i\alpha_s(\mathcal{B}_+e^{-i\Lambda_p x}+\mathcal{B}_-e^{+i\Lambda_p x})=0,$$

$$e^{\mp i\Lambda_p x}\frac{\partial\mathcal{B}_\pm}{\partial x}\mp i\alpha_p(\mathcal{A}_+e^{-i\Lambda_s z})+\mathcal{A}_-e^{+i\Lambda_s z})=0. \tag{5}$$

The wave coupling parameter $\alpha_{s,p}$ [11,12], when only one metal plate is corrugated, can be presented as

$$\alpha_{s,p}=\frac{\omega a_1}{8\pi N_{s,p}}(\vec{H}_{st}\vec{H}_{pr}+\vec{E}_{sn}\vec{E}_{pn}), \tag{6}$$

where $\vec{H}_\tau, E_n$ are the tangential component of the magnetic field and the normal component of the electric field at an unperturbed surface of the planar waveguide, respectively,

$$N_j=\left|\frac{c}{2\pi}\int\vec{E}_{\perp j}\vec{H}_{\perp j}dy\right|=\frac{\varepsilon_j h_j\omega a_0}{4\pi}$$

is the wave norm ($\varepsilon_j=2$ for a TEM mode and $\varepsilon_j=1$ for other modes), and $\Lambda_s=h_s-\bar{h}_z$, $\Lambda_p=h_p-\bar{h}_x$ are the spatial mismatches from Bragg resonance.

The conditions $\Lambda_{s,p}=0$ determine the Bragg frequency ω_0 (i.e., the frequency of the precise Bragg resonance). For given geometric parameters of the resonator including the corrugation period d and the distance between the plates a_0, this frequency satisfies the relation

$$\frac{\omega_0}{c}=\sqrt{\bar{h}^2\cos^2\varphi+g_s^2}=\sqrt{\bar{h}^2\sin^2\varphi+g_p^2}. \tag{7}$$

The frequencies of eigenmodes in the resonator may be shifted from the Bragg frequency. Assuming $\omega=\omega_0(1+\Omega)$, where $|\Omega|\ll 1$, and taking into account Eq. (7) we have for the spatial mismatches

$$\Lambda_{s,p}=\nu_{s,p}\Omega,$$

where $\nu_s=\omega_0^2/\bar{h}c^2\cos\varphi$ and $\nu_p=\omega_0^2/\bar{h}c^2\sin\varphi$. Introducing new variables

$$A_\pm=\sqrt{N_s\nu_s}\mathcal{A}_\pm e^{\mp i\Lambda_s z},\quad B_\pm=\sqrt{N_p\nu_p}\mathcal{B}_\pm e^{\mp i\Lambda_p x},$$

$$Z=z\sqrt{\nu_s/\nu_p}=z\sqrt{tg\varphi},\quad X=x\sqrt{\nu_p/\nu_s}=x\sqrt{ctg\varphi},$$

$$\delta=\Omega\sqrt{\nu_s\nu_p}$$

it is possible to simplify Eq. (5) and reduce it to the form

$$\frac{\partial A_\pm}{\partial Z}\mp i\delta A_\pm \pm i\alpha(B_+ + B_-)=0,$$

$$\frac{\partial B_\pm}{\partial X}\mp i\delta B_\pm \pm i\alpha(A_+ + A_-)=0. \tag{8}$$

The wave coupling parameter in Eqs. (8), $\alpha=\alpha_s\sqrt{N_s/N_p}=\alpha_p\sqrt{N_p/N_s}$, may be rewritten using Eqs. (6) and (3) as

$$\alpha=\frac{a_1\sqrt{h_s h_p}}{2a_0\sqrt{\varepsilon_s\varepsilon_p}} \tag{9a}$$

for mutual scattering of the ''s'' wave of TM type into the ''p'' wave of TM type and

$$\alpha=\frac{\omega a_1 g_s}{2a_0 c\sqrt{h_s h_p}\sqrt{\varepsilon_p}} \tag{9b}$$

for mutual scattering of the ''s'' wave of TE type into the ''p'' wave of TM type. As it follows from Eq. (6), the coupling of two waves of TE type on the Bragg structure is negligibly small (in the approximation proportional to $\overline{ha}_1$) because the normal component of the electric field E_n tends to zero on the corrugated surface and the magnetic field vectors $\vec{H}_\tau$ are perpendicular to each other.

Note that the TM and TEM waves for which $\vec{E}\|\vec{y}_0$ can be used in FEM's with guide magnetic fields and cyclotron autoresonance masers (CARM's). For planar FEM's without guide magnetic fields only TE waves can be used as operating ones, because for these waves $\vec{E}\|\vec{x}_0$, which makes interaction possible with the electrons oscillating along the x coordinate. In such a case the 2D feedback may be provided by scattering of the TE ($\mathcal{A}_\pm$) and TM ($\mathcal{B}_\pm$) waves.

To obtain a high Doppler up-shift for all the types of the devices mentioned above, the phase velocity of the wave interacting with the electrons (let us further assume that this is a partial wave $\mathcal{A}_+$) should be close to the speed of light. Hence, this wave should propagate at a small angle with respect to the electron-beam motion direction and should be one of the lowest modes of the waveguide. Meanwhile, the partial waves $\mathcal{B}_\pm$, which are responsible for the transverse energy fluxes over the x coordinate, can be chosen by propagating at a large angle to the axis and having smaller group velocities. Accordingly to Eq. (9b), decreasing the group velocity of $\mathcal{B}_\pm$, one can increase the distance between plates a_0 keeping the wave coupling coefficient a constant. This way it is possible for TM waves to retain the selective properties of the resonator while increasing the transverse size of the resonator in the y direction (compare with [13]). It should be noted that the limitation along this direction (y direction) is the same as for other microwave oscillators, which use traditional 1D Bragg resonators.

III. EIGENMODES OF THE OPEN 2D BRAGG RESONATOR

Let us find the frequencies, Q factors, and spatial structures for eigenmodes of the open 2D Bragg resonator [Fig. 1(a)]. Assuming that fluxes of electromagnetic energy from outside are absent and that the partial waves do not reflect from the end of the corrugated surface, the boundary conditions for Eq. (8) can be written as

$$A_+\left(X,-\frac{L_z}{2}\right)=0,\quad A_-\left(X,\frac{L_z}{2}\right)=0, \tag{10a}$$

$$B_+\left(-\frac{L_x}{2},Z\right)=0,\quad B_-\left(\frac{L_x}{2},Z\right)=0, \tag{10b}$$

where $L_z=l_z\sqrt{tg\varphi}$ and $L_x=l_x\sqrt{ctg\varphi}$.

It is useful to introduce new variables $\{A_+(X,Z)+A_-(X,Z)\}$ and $\{B_+(X,Z)+B_-(X,Z)\}$ to reduce Eqs. (8) to the following form:

$$\frac{\partial^2}{\partial Z^2}\{A_+ + A_-\}+\delta^2\{A_+ + A_-\}=-2\alpha\delta\{B_+ + B_-\}, \tag{11a}$$

$$\frac{\partial^2}{\partial X^2}\{B_+ + B_-\}+\delta^2\{B_+ + B_-\}=-2\alpha\delta\{A_+ + A_-\} \tag{11b}$$

with the boundary conditions

$$\frac{\partial}{\partial Z}\{A_+ + A_-\}\pm i\delta\{A_+ + A_-\}\big|_{Z=\pm L_z/2}=0,$$

$$\frac{\partial}{\partial X}\{B_+ + B_-\}\pm i\delta\{B_+ + B_-\}\big|_{X=\pm L_x/2}=0. \tag{12}$$

Solutions of Eqs. (11) and (12) may be found by using separation of variables:

$$A_+(X,Z)+A_-(X,Z)=C_1 f_x(X) f_z(Z),$$

$$B_+(X,Z)+B_-(X,Z)=C_2 f_x(X) f_z(Z), \tag{13}$$

where $C_{1,2}$ are arbitrary constants and $f_{x,z}$ are the eigenfunctions of the operators $T_{x,z}$ defined as

$$T_\xi f(\xi)=\frac{d^2}{d\xi^2}f(\xi)+\delta^2 f(\xi). \tag{14}$$

The eigenfunction $f_\xi(\xi)$ of the operator T_ξ satisfying the equation $T_\xi f_\xi(\xi)=\gamma_\xi f_\xi(\xi)$ and the boundary conditions

$$\frac{d}{d\xi}f_\xi(\xi)\pm i\delta f_\xi(\xi)\big|_{\xi=\pm L_\xi/2}=0 \tag{15}$$

can be written in the following form:

$$f_\xi(\xi)=\frac{\sqrt{\delta+\lambda_\xi}}{\sqrt{\delta-\lambda_\xi}}[(\delta+\lambda_\xi)\exp(i\lambda_\xi\xi)\exp(i\lambda_\xi L_\xi) -(\delta-\lambda_\xi)\exp(-i\lambda_\xi\xi)], \tag{16}$$

where $\lambda_\xi=\sqrt{\delta^2-\gamma_\xi}$ and γ_ξ is the eigennumber of the operator T_ξ and is determined by the characteristic equation

$$\exp(2i\lambda_\xi L_\xi)=\frac{(\delta-\lambda_\xi)^2}{(\delta+\lambda_\xi)^2}. \tag{17}$$

It should be noted that it is possible to prove that the set of the eigenfunctions f_ξ is complete.

Having substituted Eq. (13) into Eq. (11), we obtain that eigennumbers γ_x,γ_z of the operators T_x and T_z are satisfying the relation

$$\gamma_z\gamma_x=4\alpha^2\delta^2, \tag{18}$$

and the characteristic equations have a form similar to Eq. (17):

$$\exp(2i\lambda_z L_z)=\frac{(\delta-\lambda_z)^2}{(\delta+\lambda_z)^2}, \tag{19}$$

$$\exp(2i\lambda_x L_x)=\frac{(\delta-\lambda_x)^2}{(\delta+\lambda_x)^2},$$

where $\lambda_{x,z}=\sqrt{\delta^2-\gamma_{x,z}}$. The joint solution of Eqs. (18) and (19) determines the spectrum of the eigenfrequencies and the Q factors of the eigenmodes of the open 2D Bragg resonator.

The spatial structures of the partial waves $A_\pm,B_\pm$ can be found by integrating Eq. (8) considering Eq. (13) and taking into account the boundary conditions (10). This leads to the following solution for the amplitudes of the partial waves $A_\pm,B_\pm$:

$$A_\pm=2i\alpha(\delta\pm\lambda_z)\exp\left[\pm i\lambda_z\frac{L_z}{2}\right]\sin\left[\lambda_z\left(Z\pm\frac{L_z}{2}\right)\right]f_x(X), \tag{20a}$$

$$B_\pm=2i\alpha(\delta\pm\lambda_x)\exp\left[\pm i\lambda_x\frac{L_x}{2}\right]\sin\left[\lambda_x\left(X\pm\frac{L_x}{2}\right)\right]f_z(Z). \tag{20b}$$

Analysis of Eqs. (18) and (19) shows that the spectrum contains high Q-factor modes

$$Q=\frac{1+\mathrm{Re}(\Omega)}{2\,\mathrm{Im}(\Omega)}\approx\frac{\sqrt{\nu_s\nu_p}}{2\,\mathrm{Im}(\delta)}\gg 1$$

under conditions of strong wave coupling $\alpha L_{x,z}\gg 1$. The eigenfrequencies of the modes are situated near the Bragg resonance $\delta\approx 0$ as well as near $\delta\approx\pm 2\alpha$ (Fig. 2) and solutions for them are given by the relations

$$\lambda_z=\frac{\pi n}{L_z}+i\frac{\pi m}{\alpha L_z L_x},\quad \lambda_x=\frac{\pi m}{L_x}+i\frac{\pi n}{\alpha L_z L_x}, \tag{21a}$$

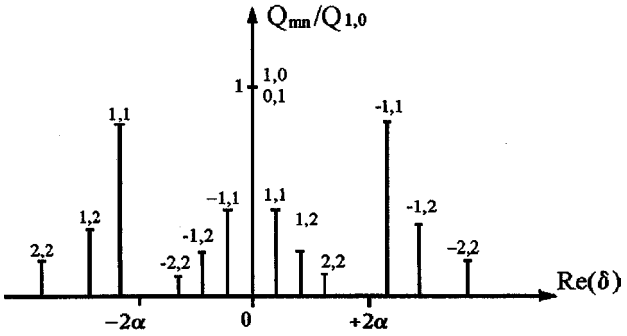

FIG. 2. The eigenmode spectrum (Q factors of the eigenmodes vs their eigenfrequencies) of the open planar 2D Bragg resonator: $L_x=L_z$.

$$\delta=-\frac{\pi^2 mn}{2\alpha L_z L_x}-i\frac{\pi^2}{2\alpha^2 L_z L_x}\left(\frac{n^2}{L_z}+\frac{m^2}{L_x}\right) \tag{21b}$$

when $\delta\approx 0$, and

$$\lambda_z=\frac{\pi n}{L_z}-is\frac{\pi n}{\alpha L_z^2},\quad \lambda_x=\frac{\pi m}{L_x}-is\frac{\pi m}{\alpha L_x^2}, \tag{22a}$$

$$\delta=\left[2\alpha+\frac{\pi^2}{4\alpha}\left(\frac{n^2}{L_z^2}+\frac{m^2}{L_x^2}\right)\right]s-i\frac{\pi^2}{2\alpha^2}\left(\frac{n^2}{L_z^3}+\frac{m^2}{L_x^3}\right) \tag{22b}$$

when $\delta\approx\pm 2\alpha$. In Eqs. (21) and (22), $n=0,\pm 1,\pm 2,\ldots$ are the longitudinal (over the z axis) and $m=0,\pm 1,\pm 2,\ldots$ are the transverse (over the x coordinate) indices of the modes, $s=\pm 1=\mathrm{sgn}(mn)$.

According to Eqs. (21) and (22), high selectivity over both the longitudinal (n) and the transverse (m) indices takes place because of output radiation (due to diffraction) not only in the longitudinal $\pm z$ directions (similar to 1D Bragg resonators), but additionally in the transverse ($\pm x$) directions. The Q factor will be maximal for the lowest modes with indices $n=0,m=1$ and $n=1,m=0$ (Fig. 2). These modes have the same eigenfrequency [$\mathrm{Re}(\delta)=0$], and when $L_x=L_z$ they have the same Q factor also. Figure 3 gives the spatial structure of the partial waves A_+ and B_- for the eigenmode $n=1,m=0$ (the structure of the A_- wave is identical to the structure of the A_+ wave and the B_- is bilaterally symmetrical to B_+). For this mode the field amplitude of the A_+ wave does not depend on the transverse x coordinate, which will provide equal energy extraction from all parts of the large electron beam. It should also be noted that the maximal amplitude of the $A_\pm$ waves is much larger than the maximal amplitude of $B_\pm$: $A_\pm^{\max}/B_\pm^{\max}=\alpha L_z$. For the mode $n=0,m=1$, the spatial structures of the partial waves $A_\pm$ and $B_\pm$ are identical to the structure of the $B_\pm$ and $A_\pm$ waves for the mode $n=1,m=0$, respectively, if we mutually exchange the z and x coordinates. For this mode $A_\pm^{\max}/B_\pm^{\max}=1/\alpha L_x$ and therefore this mode has a fairly low amplitude of the wave A_+. As A_+ is assumed to be the only partial wave resonant with the electrons, the mode $n=1,m=0$ will not be readily excited by the electron beam.

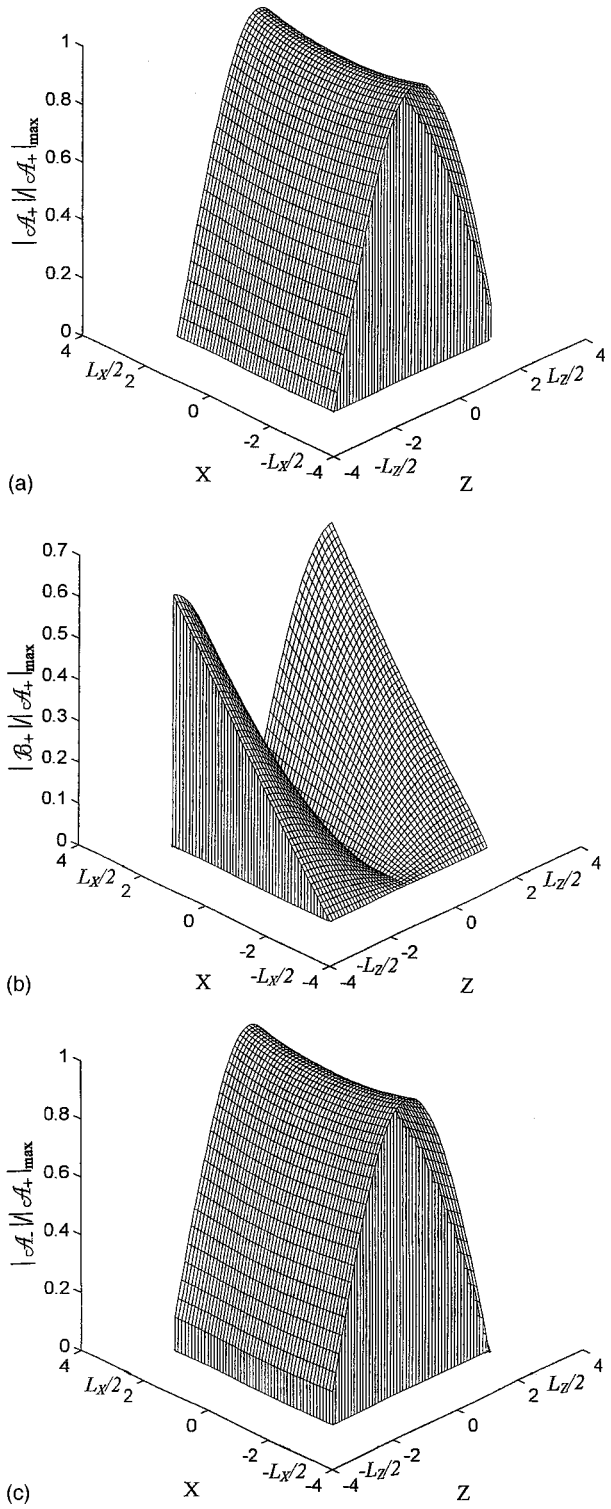

FIG. 3. Spatial structure of fundamental mode $n=1, m=0$ (with the highest Q factor) for the open planar 2D Bragg resonator ($\alpha L_x=\alpha L_z=5$): (a) normalized partial wave $\mathcal{A}_+$, (b) normalized partial wave $\mathcal{B}_+$, (c) normalized partial wave $\mathcal{A}_0$.

IV. BUILD-UP OF OSCILLATIONS IN A FEL WITH A 2D BRAGG RESONATOR

Let us investigate excitation of an open 2D Bragg resonator by a sheet relativistic electron beam. Suppose that electrons oscillate either in a periodic wiggler field (FEM) or in a uniform axial magnetic field (CARM). Let us assume that the sheet electron beam is thin and moving near a wiggler axis and let us neglect the inhomogeneities in the undulator and RF fields as well as nonuniformities of the beam, initial velocity spread, etc. As we assumed above, only the $\mathcal{A}_+$ wave is resonant with the electron beam and the resonance condition can be written in the form

$$\omega - h\nu_\parallel = \Omega, \tag{23}$$

where $\nu_\parallel = \beta_\parallel c$ is the axial electron velocity and Ω is the frequency of electron oscillations (for FEM, $\Omega=\Omega_b = 2\pi\nu_\parallel/d_w$ is the frequency of bounce oscillation in a wiggler of period d_w; for the CARM, $\Omega=\Omega_H = eH_0/\gamma mc$ is the gyrofrequency of rotation in a uniform axial field H_0 and γ is the relativistic mass factor). As a result, the resonant forward wave $\mathcal{A}_+$ may be amplified by the electron beam. On the grating it scatters into waves $\mathcal{B}_\pm$, which propagate in the transverse directions and synchronize radiation from the different parts of the electron beam (after further transformation into the wave $\mathcal{A}_+$). Simultaneously, the waves $\mathcal{B}_\pm$ scatter into the backward wave $\mathcal{A}_-$, thus completing the feedback cycle.

Let us suggest for simplicity here that the angle between the grating vectors [Fig. 1(c)] is equal to $\pi/2$, which corresponds to the case when all partial waves have the same transverse index and the same group velocities $\beta_{\rm gr}$. In this case the excitation of a 2D Bragg resonator by the electron beam and the build-up of oscillations can be described by the following system of equations [10,14]:

$$\left(\frac{\partial}{\partial Z}+\frac{1}{\beta_{\rm gr}}\frac{\partial}{\partial\tau}\right)\hat{A}_+ + i\hat{\alpha}(\hat{B}_+ + \hat{B}_-) = J,$$

$$J=\frac{1}{\pi}\int_0^{2\pi} e^{-i\theta}d\theta_0, \tag{24a}$$

$$\left(-\frac{\partial}{\partial Z}+\frac{1}{\beta_{\rm gr}}\frac{\partial}{\partial\tau}\right)\hat{A}_- + i\hat{\alpha}(\hat{B}_+ + \hat{B}_-) = 0, \tag{24b}$$

$$\left(\pm\frac{\partial}{\partial X}+\frac{1}{\beta_{\rm gr}}\frac{\partial}{\partial\tau}\right)\hat{B}_\pm + i\hat{\alpha}(\hat{A}_+ + \hat{A}_-) = 0, \tag{24c}$$

$$\left(\frac{\partial}{\partial Z}+\frac{1}{\beta_\parallel}\frac{\partial}{\partial\tau}\right)^2\theta = \mathrm{Re}(\hat{A}_+ e^{j\theta}). \tag{24d}$$

The boundary conditions for the partial waves in Eqs. (24) keep the form (10) and the boundary conditions for the monoenergetic, unmodulated electron beam take the form

$$\theta|_{Z=L_z/2}=\theta_0\in[0,2\pi), \quad \left(\frac{\partial}{\partial Z}+\frac{1}{\beta_\parallel}\frac{\partial}{\partial\tau}\right)\theta\Big|_{Z=-L_z/2}=\Delta. \tag{25}$$

Here we have used the following dimensionless variables and parameters:

$$Z=(\omega_0/c)zC, \quad X=(\omega_0/c)xC,$$

$$\tau=\omega_0 tC, \quad \hat{\alpha}=\alpha c/\omega_0 C,$$

$$(\hat{A}_\pm,\hat{B}_\pm)=e\kappa\mu(\mathcal{A}_\pm,\mathcal{B}_\pm)/mc\omega_0\gamma_0 C^2,$$

$$\Delta=(\omega_0-h\nu_\parallel-\Omega)/\omega_0 C$$

is the initial mismatch from resonance, $\theta=\omega_0 t-hz-\int\Omega\,dt$ is the electron phase with respect to the resonant wave, θ_0 is the initial electron phase,

$$C=\left(\frac{e\hat{I}_0}{mc^3}\frac{\lambda^2\kappa^2\mu}{8\pi\gamma_0 a_0}\right)^{1/3}$$

is the gain parameter, $k\approx\beta_\perp/2\beta_\parallel$ is the parameter describing coupling between the wave and electrons, μ is the inertial bunching parameter ($\mu\approx\gamma_0^{-2}$ for a FEM and $\mu\approx 1-\beta_{\rm ph}^{-2}$ for a CARM), $\hat{I}_0$ is the unperturbed electron current per unit transverse size, $\beta_{\rm ph}$ is the phase velocity of the synchronous wave, and $L_{x,z}=l_{x,z}C\omega_0/c$. The electron efficiency is given by the relations

$$\eta=\frac{C}{\mu(1-\gamma_0^{-1})}\hat{\eta},$$

$$\hat{\eta}=\frac{1}{2\pi L_x}\int_{-L_x/2}^{+L_x/2}dX\int_0^{2\pi}\left(\frac{\partial\theta}{\partial Z}-\Delta\right)\Big|_{Z=+L_x/2}d\theta_0. \quad (26)$$

Time dependencies of the efficiency in the range of the parameters where the establishment of a stationary regime of oscillation takes place are presented in Fig. 4(a). Note that in the numerical simulations we assumed $\beta_\parallel=\beta_{\rm gr}$. In the stationary regime the spatial structures of the partial waves $\mathcal{A}_\pm$ and $\mathcal{B}_\pm$ are close to the structures of the corresponding waves for the highest-Q (fundamental) mode $n=1,m=0$ of the cold resonator (compare Fig. 5 and Fig. 3). As it is seen from the spectrum of output radiation $S_\Omega=\int_0^{+\infty}\hat{A}_+(\tau,Z=L_z/2)e^{i\Omega\tau}d\tau$, the oscillation frequency coincides with the frequency of this mode, i.e., with the Bragg frequency [Fig. 4(b)]. The self-excitation condition (see the Appendix for details) for this mode may be presented in the form

$$P=\hat{\alpha}^2 L_x L_z^4\geqslant 250,\quad \Delta L_z\approx\pi. \quad (27)$$

It is important to note that the transverse distribution of the amplitude of the resonant wave $\mathcal{A}_+$ does not depend on the transverse coordinate x, thus providing equal energy extraction for all parts of the electron beam.

The principal problem for the scheme of FEM considered here is the question regarding the maximum transverse width of the system (l_x) under which the regime of spatial synchronization of radiation from different parts of the electron beam can be realized. From the set of Eqs. (24) it may be found that in the steady-state generation regime ($\partial/\partial\tau=0$), when the fundamental mode $n=1,m=0$ is excited, the dependencies of waves $\mathcal{B}_\pm$ on the transverse coordinate may be presented as

$$\hat{B}_+=\hat{\alpha}X(\hat{A}_++\hat{A}_-),\quad \hat{B}_-=\hat{\alpha}(L_x-X)(\hat{A}_++\hat{A}_-). \quad (28)$$

This allows us to reduce Eqs. (24) to the form

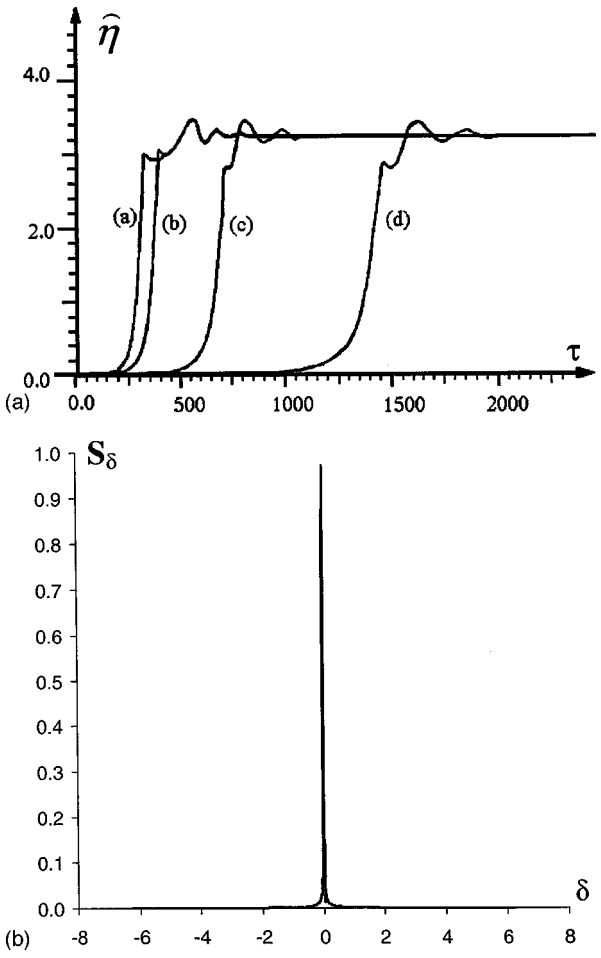

FIG. 4. Establishment of the stationary regime of oscillations in a FEL with the open planar 2D Bragg resonator: (a) Dependence of the normalized efficiency on time when $L_z=4$, $\Delta=-1.82$, $\hat{\alpha}^2L_x=1.25$, and (a) $-L_x=0.8$, $\hat{\alpha}=1.25$; (b) $-L_x=3.2$, $\hat{\alpha}=0.625$; (c) $-L_x=12.8$, $\hat{\alpha}=0.315$; (d) $-L_x=28.8$, $\hat{\alpha}=0.208$. (b) Spectrum of output radiation in the stationary regime of oscillation when $L_x=12.8$, $\hat{\alpha}=0.315$.

$$\frac{d\hat{A}_+}{dZ}+i\hat{\alpha}^2L_X(\hat{A}_++\hat{A}_-)=\frac{1}{\pi}\int_0^{2\pi}e^{-i\theta}d\theta_0,$$

$$\frac{d\hat{A}_-}{dZ}-i\hat{\alpha}^2L_x(\hat{A}_++\hat{A}_-)=0, \quad (29)$$

$$\frac{d^2\theta}{dZ^2}=\mathrm{Re}(\hat{A}_+e^{i\theta}).$$

Therefore, if the system length is constant, $L_z=\mathrm{const}$, the distribution of the waves along the longitudinal coordinate as well as the efficiency do not change when the condition $\hat{\alpha}^2L_x=\mathrm{const}$ is satisfied. Such a scaling gives us the possibility of increasing the width of the interaction space L_x while simultaneously decreasing the coupling parameter (for example, decreasing the corrugation depth α_1). Computer simulation of the nonstationary equations (24) confirms this conclusion. If $L_z\leqslant 5$, the synchronization regime is stable at least up to $L_x\leqslant 30$ (that for a gain parameter $C\approx 5\times10^{-3}$

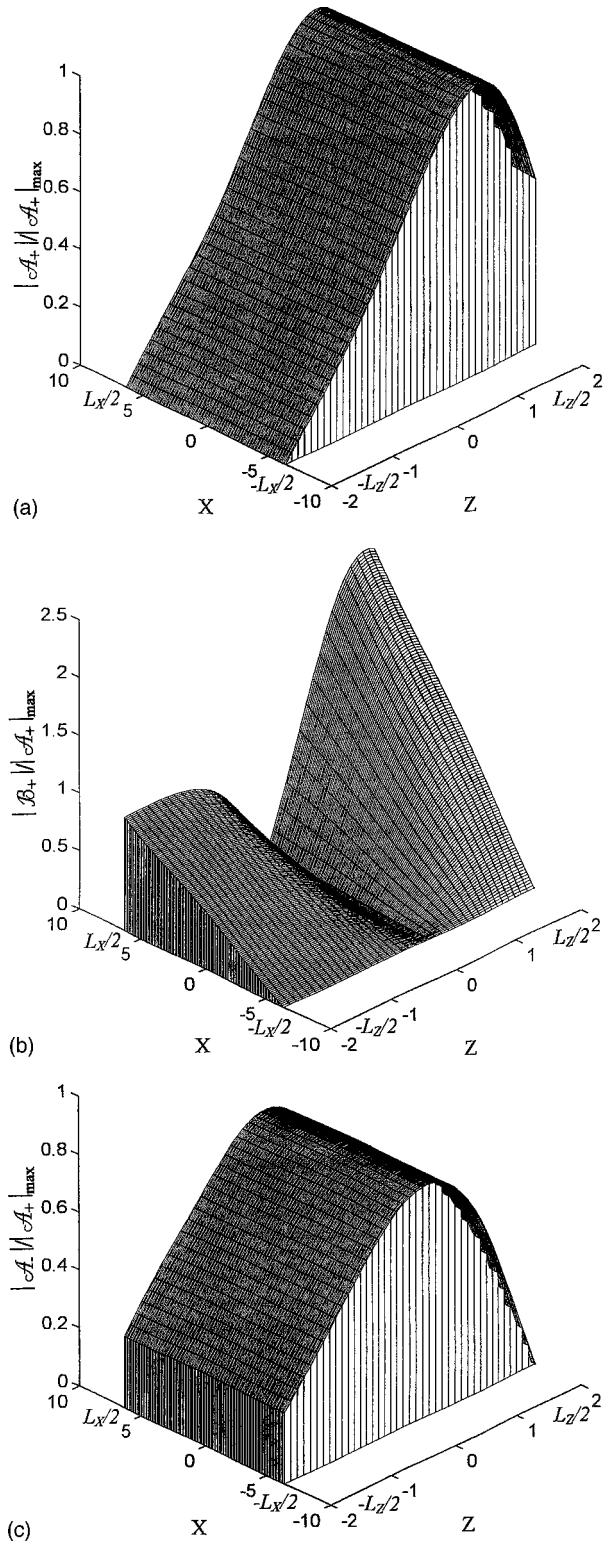

FIG. 5. Spatial structures of the partial waves' amplitudes in the stationary regime of oscillations when $L_z=4$, $\Delta=-1.82$, $L_x=12.8$, $\hat{\alpha}=0.315$. (a) Normalized partial wave $\mathcal{A}_+$, (b) normalized partial wave $\mathcal{B}_+$, (c) normalized partial wave $\mathcal{A}_-$.

corresponds to $L_x/\lambda \approx 10^3$). However, the transient time increases with the increase in the system width [Fig. 4(a)].

It should be noted that a stable single-frequency oscillation regime corresponds to excitation of the fundamental wave realized when the threshold condition $P \geqslant 250$ is moderately exceeded. Increasing this parameter, an excitation of other modes was observed. In particular, an excitation of the eigenmode $n=m=1$ was obtained when the conditions

$$\hat{\alpha}^2 L_x^2 L_z^4/(L_x+L_z) \geqslant 500, \quad (\Delta \pm 2\hat{\alpha})L_z \approx \pi \tag{30}$$

were satisfied. When P greatly exceeds the threshold, multifrequency self-modulation regimes of generation were realized. In this case the spatial structures of output radiation exhibited periodical or chaotical variations with time.

V. INFLUENCE OF SIDE REFLECTIONS ON THE SELECTIVE PROPERTIES OF A 2D BRAGG RESONATOR

As was shown in the preceding section, a 2D Bragg resonator open in the transverse direction displays practically unlimited possibilities for increasing the system's transverse size. However, in practice it is rather difficult to realize extraction of energy from all directions especially in the scheme of FEM's where a guide magnetic field produced by a solenoid is employed. It is possible to suggest several solutions how to provide a singly directed output of radiation. One of them is to use additional reflectors situated outside the interaction space in order to turn the transverse energy fluxes into the longitudinal direction. However, it is much more simple to restrict the 2D Bragg resonator by two metal mirrors on the transverse edges [Fig. 1(b)]. Such a closed system in the transverse directions will possess less selectivity than the original open one, while under certain conditions a single mode operation regime can be achieved. Thus, in this section we consider the influence of side reflections on the operability of a FEM with two-dimensional feedback.

In the case of arbitrary reflections from the transverse edge of the resonator, the boundary conditions for Eq. (8) remain the same [i.e., Eq. (10a)] for the longitudinal e.m. fluxes, but for the transverse e.m. fluxes they take the form

$$B_+\left(-\frac{L_x}{2},Z\right)=RB_-\left(-\frac{L_x}{2},Z\right),$$

$$B_-\left(\frac{L_x}{2},Z\right)=RB_+\left(\frac{L_x}{2},Z\right), \tag{31}$$

where R is the reflection coefficient. The solution of Eq. (8) with the boundary conditions (10a) and (31) may be found by separation of variables and using new variables in the form of Eq. (13). In this case the functions $\tilde{f}_x$ are the eigenfunctions of the operator $\tilde{T}_x$ given by the same equation (14) but with the modified boundary conditions

$$\left(\frac{1+R}{1-R}\right)\frac{\partial}{\partial X}\{B_+ + B_-\} \pm i\,\delta\{B_+ + B_-\}\Big|_{X=\pm L_x/2}=0. \tag{32}$$

A new set of the eigennumbers $\delta, \gamma_z, \tilde{\gamma}_x$ [where γ_z is the eigennumber of the operator T_z given by Eqs. (14) and (15) and $\tilde{\gamma}_x$ is the eigennumber of the operator $\tilde{T}_x$ given by Eqs. (14) and (32)] should be yielded by the joint solution of the characteristic equations

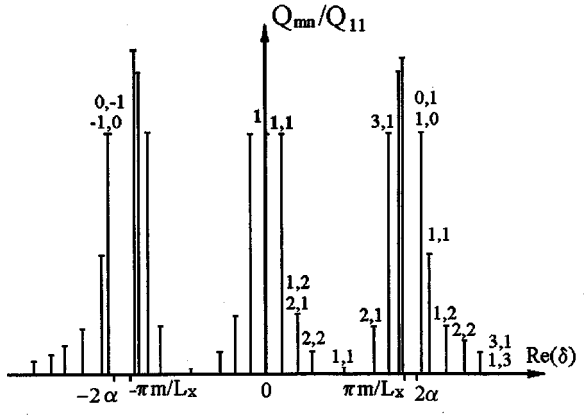

FIG. 6. The spectrum of eigenfrequencies and Q factors of the modes for closed (side reflection $R=-1$) planar 2D Bragg resonator: $L_x=L_z$.

$$\exp(2i\lambda_z L_z)=\frac{(\delta-\lambda_z)^2}{(\delta+\lambda_z)^2}, \tag{33a}$$

$$\exp(2i\lambda_x L_x)=\frac{[(1-R)\delta-(1+R)\lambda_x]^2}{[(1-R)\delta+(1+R)\lambda_x]^2}, \tag{33b}$$

where $\lambda_z=\sqrt{\delta^2-\gamma_z}$, $\lambda_x=\sqrt{\delta^2-\tilde{\gamma}_x}$, and the relation between the eigennumbers $\gamma_z\tilde{\gamma}_x=4\alpha^2\delta^2$ keeps the form similar to Eq. (18). Note that these equations reduce to the form of Eqs. (18) and (19) for the case of an open resonator ($R=0$).

In the case of a resonator restricted by ideal metal mirrors on the transverse sides ($R=-1$) the characteristic equation (33b) takes the form

$$\exp(2i\lambda_x L_x)=1. \tag{34}$$

The joint solution of Eqs. (18), (33a), and (34) presents three groups of eigenmodes which are situated near $\delta\approx 0$, $\delta\approx\pm 2\alpha$, and $\delta\approx\pi m/L_x$ (Fig. 6). Under the assumption of strong wave coupling they are given by the relations

$$\delta=\frac{\pi^2 nm}{2\alpha L_x L_z}-i\frac{\pi^2 m^2}{2\alpha^2 L_z L_x^2} \tag{35a}$$

at $\delta\approx 0$,

$$\delta=\pm\left[2\alpha+\frac{\pi^2}{4\alpha}\left(\frac{n^2}{L_z^2}+\frac{m^2}{L_x^2}\right)\right]-i\frac{\pi^2 n^2}{2\alpha^2 L_z^3} \tag{35b}$$

at $\delta\approx\pm 2\alpha$,

$$\delta=\frac{\pi m}{L_x}\left(1-\frac{2\alpha^2 L_z^2}{\pi^2 n^2}\right)-i\frac{2\alpha^2 L_z^3 m^2}{\pi^2 n^4 L_x^2}, \tag{35c}$$

at $\delta\approx\pi m/L_x$, where m and n are the transverse and the longitudinal indices of the modes, respectively. The eigenfunctions of the operator $\tilde{T}_x$ for $R=-1$ have the form

$$\tilde{f}_x(X)=\exp\left(-i\lambda_x\frac{L_x}{2}\right)\sin\left[\lambda_x\left(X+\frac{L_x}{2}\right)\right]. \tag{36}$$

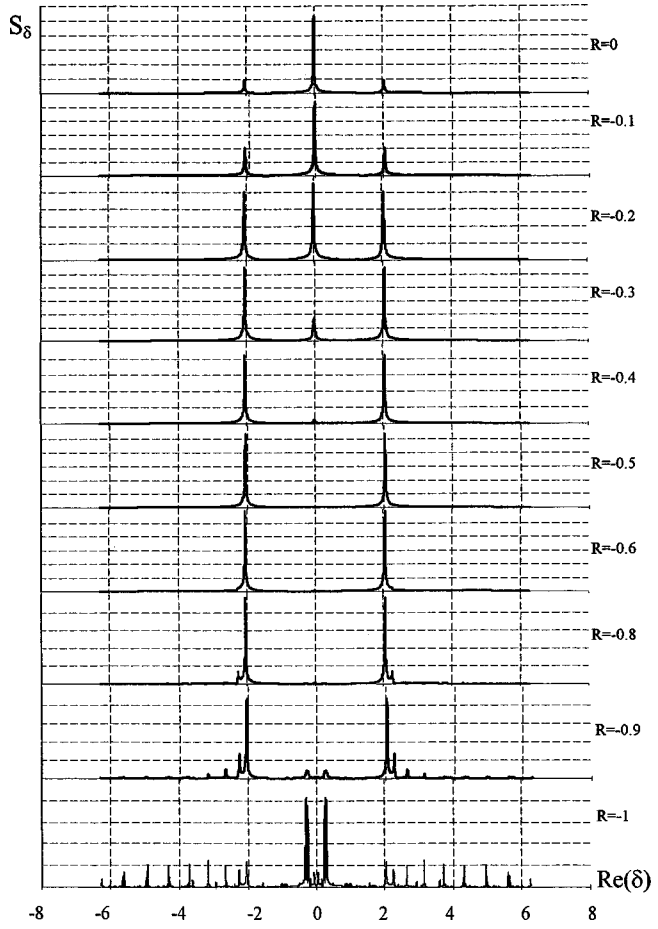

FIG. 7. Evolution of the mode spectrum of the planar 2D Bragg resonator ($\alpha L_x=\alpha L_z=9$) vs side reflection coefficient R.

The relation (36) shows that the eigenmode at the frequency of exact Bragg resonance $\delta\equiv 0$ is not present in the spectrum of the closed resonator. At the same time a new set of eigenmodes having frequencies $\delta\approx\pi m/L_x$ arises compared with those of the open resonator. Under the zero wave coupling condition $\alpha=0$ on the Bragg gratings (zero corrugation depth) these eigenmodes are reduced to the eigenmodes of a two-mirror resonator formed by the metal side walls. For this set of modes an increase of the wave coupling (α) results in an increase of the scattering of the transverse propagating waves into the longitudinal propagating ones and increases diffraction losses. Thus, the Q factors of these modes decrease with the increase of α (in contrast to the behavior of modes located near $\delta\approx 0$ and $\delta\approx\pm 2\alpha$, which originate from scattering of the waves on the Bragg structure). At $\alpha\neq 0$, the Q factors of the eigenmodes from all sets of modes are comparable to each other and, as a result, the selective properties of the cold resonator are impaired.

For an arbitrary R the evolution of the resonator's spectrum versus the reflection coefficient is shown in Fig. 7. This spectrum is obtained from simulation using a time-domain code which solves Eqs. (24) with boundary conditions (10a) and (31) under the assumption of absence of the electrons (i.e., zero beam current $J=0$). Some arbitrary initial field distribution was assumed at $\tau=0$ for this code and the mode spectrum was plotted for τ significantly exceeding the time for the waves to complete the feedback cycle of the resonator

(i.e., $\tau \geqslant 10^3$ for parameters presented in Fig. 7), when the mode spectrum practically has no dependence on the initial field distribution. This method allows one to separate the highest Q-factor modes presented in the spectrum. Figure 7 shows that for $|R| \leqslant 0.2$ the spectrum of eigenfrequencies is close to the spectrum of the open resonator. The resonator retains high selectivity over the longitudinal and the transverse coordinates with the maximum Q factor belonging to the eigenmode at the Bragg resonance frequency. The Q factor of this mode decreases with an increase of the reflection coefficient and at $0.3 < |R| < 0.8$ the eigenmodes with one field variation over both the transverse and longitudinal coordinates ($|m| = |n| = 1$) located at $\delta \approx \pm 2\alpha$ have the highest Q factor. At $R \approx -1$, there are a few sets of eigenmodes in the spectrum of the cold resonator with the Q factors at the same level.

To study the excitation of the resonator by the electron beam for $R \neq 0$, the system of Eq. (24) with the boundary conditions (10a), (25), and (31) was solved. The numerical simulations of oscillation build-up in the resonator with small side reflections ($|R| \leqslant 0.3$) demonstrate the existence of a broad range of the system's parameters where the single-mode operation regime is established practically for any width of the resonator. In this case, similar to the open resonator, the fundamental mode at the Bragg frequency with approximately constant transverse distribution is excited by the beam.

For high reflectivity from the transverse side walls ($R \approx -1$), the single-mode operation regime is changed to the self-modulation regime for large widths of the resonator $L_x \geqslant 10$. These regimes are accompanied by excitation of several modes of the resonator, of which beating takes place [Fig. 8(a)]. However, for $L_x \leqslant 7$ the single-mode operating regime may be realized even in the closed resonator when $R = -1$ [Fig. 8(b)]. The establishment of the single-mode operating regime is caused by electronic selection of the different modes [15,16] (as opposed to electrodynamical mode selection in the open 2D Bragg resonator). The field structure of the partial wave resonant with the electron beam in the steady-state operating regime is now dependent on the x coordinate but it still has the convenient amplitude field distribution for interaction with the electron beam (Fig. 9). It should be noted that even small RF losses for the transverse e.m. fluxes (i.e., decrease in reflection from the transverse side walls) stabilize the single-mode operation of the FEL (Fig. 10).

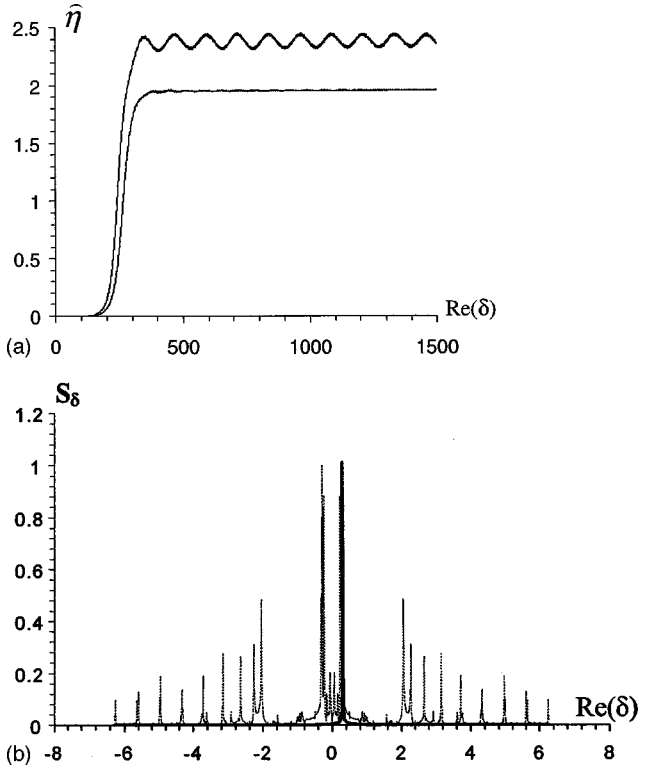

FIG. 8. Oscillation build-up in a FEL with the closed planar 2D Bragg resonator: (a) Time dependence of the normalized efficiency for $L_z = 3$, $R = -0.99$, $\Delta = -2.3$, and $1 - L_x = 10, \hat{\alpha} = 0.4$; $2 - L_x = 7, \hat{\alpha} = 0.5$. (b) Spectrum of output radiation in the stationary regime of oscillation (solid line) for $L_z = 3$, $L_x = 7$, $R = -0.99$, $\Delta = -2.3$, $\hat{\alpha} = 0.5$, and spectrum of eigenmodes with the highest Q factor of the ''cold'' resonator with the same geometrical parameters (dashed line).

VI. DESIGN OF A HIGH-POWER FEM DRIVEN BY A SHEET ELECTRON BEAM

Experimental study of a powerful millimeter wavelength FEM driven by a sheet electron beam has been carried out using the high-current microsecond accelerator U-2 (INP RAS, Novosibirsk). In recent experiments a scaled down sheet electron beam with particle energy of 1 MeV, beam current of 4 kA, and cross section of 0.3 cm$\times$12 cm was used. A conventional planar two-mirror Bragg resonator provided selective 1D distributed feedback at the 4 mm operating wavelength. As a result of the experiments, an output power of 200 MW in a microwave pulse of 1 μs duration was obtained [17]. Thus, even at the present stage, a record energy per pulse for millimeter wavelength generators of 200 J has been achieved.

Further increases in the radiation power can be achieved by using the full-scale beams with cross section 0.5 cm$\times$140 cm (energy content about 80 kJ) and 3 cm$\times$140 cm (energy content up to 0.4 MJ) which are generated by the U-2 accelerator. The theoretical analysis described in this paper has demonstrated the potential of 2D Bragg resonators in obtaining high-power spatially coherent radiation from such a wide beam.

Let us consider here an FEM project using the 2D Bragg resonators to generate radiation of wavelength $\lambda = 4$ mm on the basis of the U-2 accelerator (1 MV/200 A/cm/5 μs/cross section 0.5 cm$\times$140 cm). Let the wiggler be of 4 cm period and the amplitude of the wiggler field be up to 0.1 T. It allows one to produce an oscillatory electron velocity $\beta_\perp \approx 0.2$–0.3 and parameter $\mu \approx \gamma^{-2} \approx 0.1$ at an axial guide field strength of about 1 T [17]. In this case, when the distance between cavity plates $a_0 = 1$ cm, the gain parameter is $C \approx 0.006$. For these parameters the dimensionless transverse size $L_x \approx 12$ [curve 3 in Fig. 4(a)] corresponds to a beam width of about 140 cm. Thus, following computer simulation, the use of an open 2D Bragg resonator with a corrugation of period 3 mm and depth 0.3 mm would make it possible to realize a single-mode-operation regime in the FEM. It will provide spatially coherent radiation when the over-

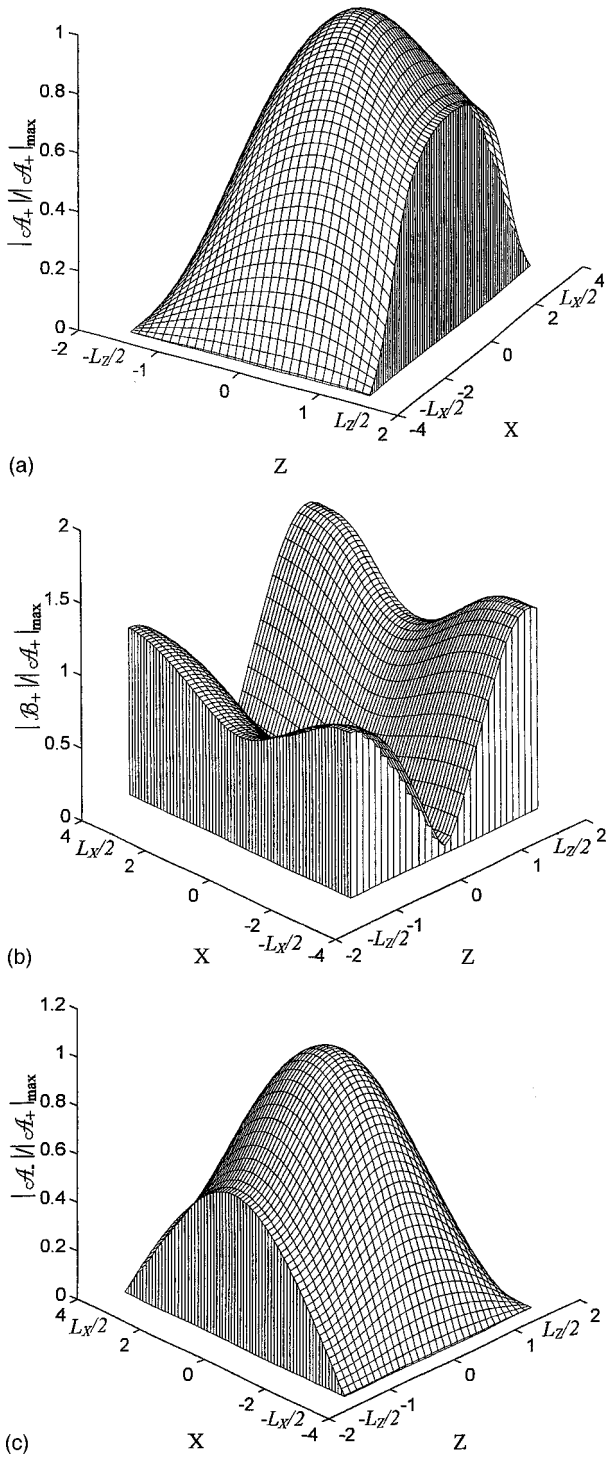

FIG. 9. Spatial structures of the partial waves amplitudes in the stationary regime of oscillations when $L_z=3$, $L_x=7$, $\Delta=-2.3$, $\hat{\alpha}=0.5$. (a) Normalized partial wave $\mathcal{A}_+$, (b) normalized partial wave $\mathcal{B}_+$, (c) normalized partial wave $\mathcal{A}_-$.

sized parameter $l_x/\lambda \approx 350$. The transit time will be about 200 ns. With the efficiency of 15% the radiation power is calculated to be 4 GW. For a full-scale beam with cross section 3 cm$\times$140 cm and beam current 1 kA/cm the gain parameter is the same when the distance between the 2D Bragg cavity plates $a_0=5$ cm. Thus, all dimensionless parameters stay the same and from curve 3 in Fig. 4(a) it may be estimated for this experiment (do not take into account all the inhomogeneity in the e-beam and fields) that output power can be as great as 20 GW.

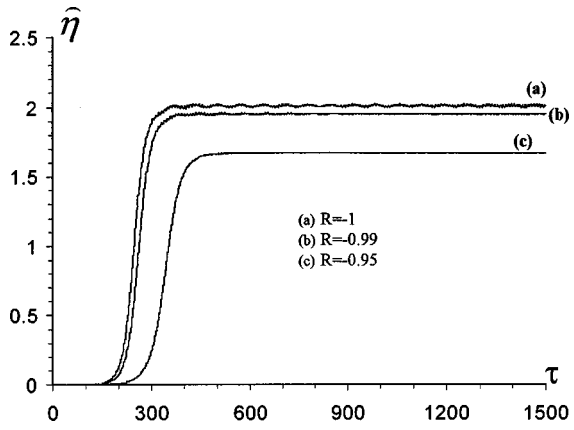

FIG. 10. Time dependence of the normalized efficiency of FEL's with planar 2D Bragg resonator for different values of the side reflection R ($L_z=3$, $L_x=7$, $\Delta=-2.3$, $\hat{\alpha}=0.5$).

At the same time, for a sheet beam of width about $l_x/\lambda \approx 100$ the simpler transversely closed resonator scheme may be used. The dimensionless transverse size $L_x \approx 7$ [curve 2 in Fig. 8(a)] corresponds to a beam width of 80 cm for FEM parameters discussed above. Following computer simulations, the FEM with a side closed resonator driven by an electron beam of width about 50–80 cm will be able to operate at a single frequency around 75 GHz. Considering the same operating parameters as for the open system, the efficiency of the FEM can be 10%. The transit time is expected to be shorter than 100 ns and the radiation power is calculated to be up to 1–2 GW for a beam of current 200 A/cm and approximately 5–7 GW for a beam of current 1 kA/cm.

ACKNOWLEDGMENTS

This work was supported in part by Grant No. 531 of the International Science and Technology Center, Grant No. 97-02-17379 of the Russian Foundation for Basic Research, and British Gas.

APPENDIX

Presented below is the self-excitation condition for a planar open 2D Bragg resonator. It may be obtained from the power balance equation

$$\frac{\omega W}{Q} = \eta I_b U_B, \tag{A1}$$

which is valid in a stationary regime of oscillation. The right side of formula (A1) represents power radiated by the electron beam of current I_b and voltage U_b, and the left side corresponds to the diffraction losses from the resonator for the mode with the frequency ω, Q factor Q, and e.m. energy storage $W=1/4\pi\int|\vec{E}^2|dV$.

Electron efficiency near a threshold of generation (i.e., in a small signal regime) may be found from equations of particle motion (24e) after linearization and implementing the sequential approximations method (see [18] for details):

$$\hat{\eta}_{st}=\frac{1}{4L_x}\int_{-l_x/2}^{l_x/2}dX\frac{d}{d\Delta}\left|\int_{-L_z/2}^{L_z/2}A_+(X,Z)e^{i\Delta Z}\,dZ\right|^2, \tag{A2}$$

where $A_+(X,Z)$ is the spatial structure of the partial wave which is in synchronism with the electrons. Substituting in Eq. (A2) the structure of the partial wave (20a) for the highest Q mode $n=1,m=0$, we come to the following formula for electron efficiency in the small signal regime:

$$\tilde{\eta}_{st}=\pi^2A_{+0}^2L_z^3\frac{d}{d\Psi}\left[\frac{1+\cos\Psi}{(\Psi^2-\pi^2)^2}\right], \tag{A3}$$

where $\Psi=\Delta L_z$ is the transit angle and A_{+0} is the partial wave amplitude. The maximum efficiency

$$\hat{\eta}_{sl}^{\max}\approx 0.04A_{+0}^2L_z^3 \tag{A4}$$

is reached at $\Psi\approx\pi$.

For the e.m. energy stored in the resonator, which is associated with excitation of the fundamental mode, from the expressions (2) and (20) we have $W\approx(1/\pi)\mathcal{A}_{+0}^2a_0l_xl_z$. As a result, from Eq. (A1) using relation (21) for the fundamental mode Q factor and Eqs. (26) and (A4) for electron efficiency and going to the dimensionless variables, we obtain the condition (27). The self-excitation condition (30) for other modes can be obtained using similar procedures.

[1] V.L. Bratman, G.G. Denisov, N.S. Ginzburg, and M.I. Petelin, IEEE J. Quantum Electron. **QE-19**, 282 (1983).

[2] M. Wang, Z. Wang, J. Chen, Z. Lu, and L. Zhang, Nucl. Instrum. Methods Phys. Res. A **304**, 116 (1991).

[3] T.S. Chu, F. Hartemann, B.G. Danly, and R.J. Temkin, Phys. Rev. Lett. **72**, 2391 (1994).

[4] P. Zambon and P.J.M. Van der Slot, Nucl. Instrum. Methods Phys. Res. A **341**, 484 (1994).

[5] N.S. Ginzburg, A.K. Kaminsky, A.A. Kaminsky, N.Yu. Peskov, S.N. Sedykh, A.P. Sergeev, and A.S. Sergeev, IEEE Trans. Plasma Sci. **26**, 536 (1998).

[6] A.V. Arzhannikov, V.S. Nikolaev, S.L. Sinitsky, and M.V. Yushkov, J. Appl. Phys. **72**, 1657 (1992).

[7] A.V. Arzhannikov, V.B. Bobylev, V.S. Nikolaev, S.L. Sinitsky, and A.V. Tarasov, *Proceedings of the 10th International Conference on High-Power Particle Beams, San Diego, 1994* [NTIS Report No. PB95-144317 (1995)], pp. 136–139.

[8] N.S. Ginzburg, N.Yu. Peskov, and A.S. Sergeev, Opt. Commun. **96**, 254 (1993).

[9] N.S. Ginzburg, N.Yu. Peskov, A.S. Sergeev, A.V. Arzhannikov, and S.L. Sinitsky, Nucl. Instrum. Methods Phys. Res. A **358**, 189 (1995).

[10] N.S. Ginzburg, N.Yu. Peskov, A.D.R. Phelps, G.R.M. Robb, and A.S. Sergeev, IEEE Trans. Plasma Sci. **24**, 770 (1996).

[11] N.F. Kovalev, I.M. Orlova, and M.I. Petelin, Izv. Vyssh. Uchebn. Zaved. Radiofiz. **11**, 783 (1968) (in Russian).

[12] G.G. Denisov and M.G. Reznikov, Izv. Vyssh. Uchebn. Zaved. Radiofiz. **25**, 562 (1982) (in Russian).

[13] V.L. Bratman *et al.*, Int. J. Electron. **59**, 247 (1985).

[14] N.S. Ginzburg, N.Yu. Peskov, A.S. Sergeev, A.V. Arzhannikov, and S.L. Sinitsky, *II-Asian Symposium on Free Electron Lasers, Novosibirsk, 1996*, edited by I. V. Pirayev (Budker Institute of Nuclear Physics, Novosibirsk, 1996), pp. 150–157.

[15] N.S. Ginzburg and M.I. Petelin, Int. J. Electron. **59**, 291 (1985).

[16] T.M. Antonsen and B. Levush, Phys. Fluids B **1**, 1097 (1989).

[17] M.A. Agafonov, A.V. Arzhannikov, N.S. Ginzburg, V.G. Ivanenko, P.V. Kalinin, S.A. Kuznetsov, N.Yu. Peskov, and S.L. Sinitsky, IEEE Trans. Plasma Sci. **26**, 531 (1998).

[18] V.L. Bratman, N.S. Ginzburg, and G.G. Denisov, Radiotekh. Elektron. **27**, 1373 (1982) (in Russian).